

RESEARCH PAPER

## An anti-HER2 antibody conjugated with monomethyl auristatin E is highly effective in HER2-positive human gastric cancer

Hongwen Li<sup>a</sup>, Chao Yu<sup>b</sup>, Jing Jiang<sup>c</sup>, Changjiang Huang<sup>b</sup>, Xuejing Yao<sup>a</sup>, Qiaoyu Xu<sup>b</sup>, Fang Yu<sup>b</sup>, Liguang Lou<sup>d</sup>, and Jianmin Fang<sup>a,e,f</sup>

<sup>a</sup>School of Life Sciences and Technology, Tongji University, Shanghai, China; <sup>b</sup>RemeGen, Ltd., Yantai, Shandong, China; <sup>c</sup>School of Pharmacy, Binzhou Medical University, Yantai, Shandong, China; <sup>d</sup>Shanghai Institute of Materia Medica, Chinese Academy of Sciences, Shanghai, China; <sup>e</sup>Tongji University Suzhou Institute, Suzhou, Jiangsu, China; <sup>f</sup>Collaborative Innovation Center for Biotherapy, West China Hospital, Sichuan University, Chengdu, Sichuan, China

### ABSTRACT

Antibody-drug conjugate (ADC) is a novel class of therapeutics for cancer target therapy. This study assessed antitumor activity of ADC with an antimitotic agent, monomethyl auristatin E (MMAE) and a humanized monoclonal anti-HER2 antibody, hertuzumab, in gastric cancer. The efficacy of hertuzumab-MC-Val-Cit-PAB-MMAE (hertuzumab-vcMMAE) on human epidermal growth factor receptor 2 (HER2) positive human gastric cancer cells, NCI-N87, was evaluated *in vitro* and *in vivo*. The cytotoxicity of hertuzumab was significantly enhanced after conjugation with MMAE. Compared to trastuzumab, hertuzumab had a higher affinity to HER2 and had more potent antibody-dependent cell-mediated cytotoxicity (ADCC) activity *in vitro*. After conjugation with MMAE, the binding specificity for HER2 was not affected. Furthermore, the internalization of hertuzumab-vcMMAE in HER2 positive gastric cancer cells was verified. Although the conjugation of hertuzumab and MMAE decreased the ADCC effect, the overall cytotoxicity was dramatically increased in HER2 positive gastric cancer cells. *In vitro* data on this hertuzumab-vcMMAE has exerted much stronger antitumor activity compared to trastuzumab-DM1 in HER2 positive gastric cancer cells. A single administration of hertuzumab-vcMMAE at 5 or 10 mg/kg showed high potency and a sustained tumor inhibitory effect on NCI-N87 xenografts in mice. In conclusion, hertuzumab-vcMMAE conjugate is a highly effective anti-HER2 targeted therapy for HER2-positive gastric cancer.

### ARTICLE HISTORY

Received 29 September 2015  
Revised 26 November 2015  
Accepted 1 January 2016

### KEYWORDS

Antibody drug conjugate;  
gastric cancer; HER2;  
monomethyl auristatin E;  
target therapy

### Introduction

Gastric cancer is one of the most common malignancies with a high mortality in a large part of the world.<sup>1</sup> Despite the steady decline in the gastric cancer mortality rate over the past 3 decades, the 5 year survival rate is still approximately 30% in the USA.<sup>2</sup> Clinically, gastric cancer is often diagnosed at the advanced stages of disease, with no curable therapies available. Radiotherapy and chemotherapy cannot effectively prolong patient survival.<sup>3</sup> Thus, there is an urgent need to develop a more effective therapy to control gastric cancer. Toward this end, molecular target therapy has become a novel anti-cancer strategy that can specifically eliminate or reduce malignant cells by discriminating tumor cells from normal cells.<sup>3</sup> This type of treatment is based on altered expression of specific oncogenes or tumor antigen in cancer cells that maintain the malignant phenotype.<sup>4</sup> For example, human epidermal growth factor receptor 2 (HER2) overexpression and gene amplification have been reported in various cancers, including breast and gastric cancers, and acts as a pro-oncogene in different human cancers.<sup>5,6</sup> HER2 belongs to human epidermal growth factor receptor (EGFR, HER) family, which includes 4 closely related members, HER1 (EGFR and ErbB1), HER2 (ErbB2), HER3

(ErbB3), and HER4(ErbB4).<sup>7–9</sup> HER2 can dimerize with other HER members to play a key role in cell signaling transduction.<sup>9</sup> Gastric cancers at advanced stages express higher levels of HER2 compared to cancers at early stages.<sup>10</sup> Although association between HER2 overexpression and prognosis of gastric cancer patients is still controversial,<sup>11–14</sup> HER2 could be a valuable target for HER2-positive gastric cancer therapy. Trastuzumab was the first anti-HER2 humanized antibody approved by the United States Food and Drug Administration (USFDA) in 1998.<sup>15</sup> Previous studies demonstrated that trastuzumab in combination with chemotherapy was highly effective compared to chemotherapy alone in HER2-positive advanced gastric or gastroesophageal junction cancer.<sup>16–21</sup> Combination of trastuzumab with another HER2 targeting monoclonal antibody also showed synergistic antitumor activity in HER2-positive gastric cancer.<sup>22</sup> Thus, targeted HER2 therapy in gastric cancer is effective, although there is still a large percentage of patients with HER2-positive gastric or breast cancer presenting with a clinical resistance to trastuzumab.<sup>17,23,24</sup>

Furthermore, the antibody-drug conjugate (ADC) is a novel class of targeting antitumor therapy that is more effective than antibodies alone and has fewer side effects, which may be due to a low concentration of free chemotherapeutic drug in the host blood

system. ADC consists of a monoclonal antibody and a highly toxic small molecule agent joined together using a small chemical linker, leading to specific delivering of the cytotoxic drug to the tumor lesion through the antibody-antigen interaction.<sup>25</sup> The first ADC drug, Mylotarg, was approved by the USFDA in 2000; although, it was later withdrawn from the market mainly due to unforeseen side effects.<sup>26</sup> Recently, the USFDA approved 2 new ADC drugs, brentuximab vedotin and trastuzumab-DM1, to treat CD30-positive Hodgkin lymphoma and systemic anaplastic large-cell lymphoma and HER2 positive metastatic breast cancer.<sup>27,28</sup> To date, a large number of ADCs are being studied in clinical trials in different stages of various hematologic or solid tumors.<sup>29</sup> Since success with brentuximab vedotin (anti-CD30 antibody conjugated with monomethyl auristatin E (MMAE)), the potent antimetabolic drug MMAE has been widely applied in many of the ADC pipelines.<sup>29</sup> According to the previous studies, therapeutic antibodies conjugated with MMAE showed high antitumor efficiency in patients with hematologic malignancies and solid tumors.<sup>30-36</sup> We utilized a humanized anti-HER2 antibody, hertuzumab, conjugated with MMAE *via* a cleavable linker to generate hertuzumab-MC-Val-Cit-PAB-MMAE (hertuzumab-vcMMAE for short). Our previous study has proven this ADC agent has a potent antitumor activity in HER2 positive breast cancer.<sup>37</sup> In this study, using preclinical models, we demonstrated that this ADC agent was highly effective in treatment of gastric cancer.

## Results

### Characteristics of hertuzumab-vcMMAE

The affinity profiles of hertuzumab, trastuzumab and hertuzumab-vcMMAE to HER2 were assessed and are illustrated in Fig. 1. Specifically, compared to trastuzumab ( $K_D = 1.86E-09$ ), hertuzumab showed a 3.7 fold higher affinity to HER2 ( $K_D = 5.02E-10$ ). After saturation with trastuzumab, the HER2-ECD still bound to hertuzumab but the affinity declined, and vice versa. This revealed that the epitope recognized by hertuzumab and trastuzumab is different but

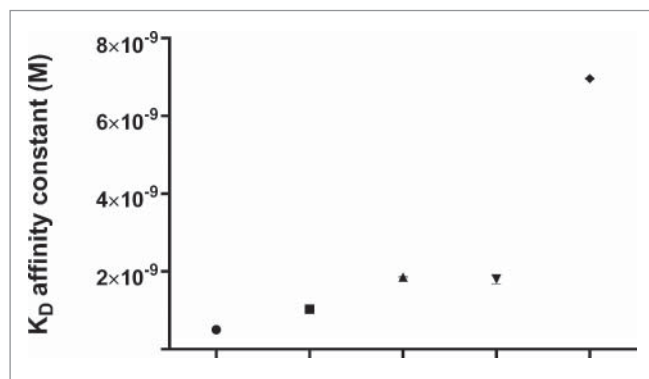


**Figure 1.** Kinetic binding analysis of Octet. Affinity constant  $K_D$  (M) for hertuzumab, trastuzumab and hertuzumab-vcMMAE binding to HER2-ECD was  $5.02 \times 10^{-10}$  (circle),  $1.86 \times 10^{-9}$  (up-pointing triangle), and  $1.03 \times 10^{-9}$  (square), respectively.  $K_D$  (M) of hertuzumab binding to trastuzumab saturated HER2-ECD was  $1.80 \times 10^{-9}$  (down-pointing triangle).  $K_D$  (M) of trastuzumab binding to hertuzumab saturated HER2-ECD was  $6.96 \times 10^{-9}$  (rhombus). The data are summarized as mean  $\pm$  SD of triplicate experiments

partially overlaps. After conjugation with MMAE, the affinity of this antibody to HER2 slightly declined with the  $K_D$  changed from  $5.02E-10$  to  $1.03E-9$ .

### Binding capacity of hertuzumab and hertuzumab-vcMMAE to HER2-positive cancer cells and clinical tumor tissues

We first performed a flow cytometry analysis to assess whether the conjugation of hertuzumab with MMAE affects the binding capacity for HER2-positive gastric cancer NCI-N87 cells (Fig. 2A). We found that this conjugate was able to bind to the cells, indicating that conjugation with MMAE did not significantly affect the antibody-antigen binding ability. Moreover, we also performed immunohistochemistry to assess the binding of this conjugate to human gastric cancer tissue specimens and found that the HER2 status in each gastric cancer tissue sample was consistent with hospital diagnosis (Fig. 2B).

### Effects of hertuzumab-vcMMAE on gastric cancer cells with HER2 expression

We then assessed the ADCC ability of hertuzumab, hertuzumab-vcMMAE, and the reference drugs (trastuzumab and trastuzumab-DM1) in NCI-N87 cells *in vitro* (Fig. 3). Our data showed that hertuzumab exhibited the strongest ADCC (effective concentration at 50% (EC50),  $<10$  ng/ml). Conjugation of hertuzumab to MMAE caused a decrease in ADCC activity (EC50 = 36 ng/ml). An opposite trend was observed in trastuzumab and T-DM1. After conjugation with DM1, the EC50 of trastuzumab changed from 29.6 to 19.6 ng/ml.

Internalization and lysosomal localization of hertuzumab-vcMMAE in NCI-N87 cells were visualized by immunofluorescence microscopy. As shown in Fig. 4, hertuzumab-vcMMAE was initially detected on the cell membrane. After incubation at 37°C for 16 h, hertuzumab-vcMMAE was internalized and the intracellular ADC signals co-localized with lysosomes.

Furthermore, we assessed the *in vitro* effects of antibody alone (hertuzumab or trastuzumab) and ADCs (hertuzumab-vcMMAE or trastuzumab-DM1) in NCI-N87 cells. The drugs inhibited growth of NCI-N87 cells in a dose-dependent manner (Fig. 5). Both hertuzumab and trastuzumab had a low inhibitory effect on NCI-N87 cells. The ADCs showed a much more potent antitumor activity than that of the antibody alone. Moreover, hertuzumab-vcMMAE (inhibitory concentration at 50% (IC50) = 95.3 ng/ml) was significantly more effective than trastuzumab-DM1 (IC50 = 568.2 ng/ml). However, in the HER2-negative gastric cancer cell line, BGC-823, hertuzumab, trastuzumab, hertuzumab-vcMMAE, trastuzumab-DM1, and the small molecule tyrosine kinase inhibitor lapatinib, showed very weak or no inhibitory effects *in vitro*. MMAE had potent antitumor activity on both HER2-positive and negative gastric cancer cell lines, indicating its poor specificity (Table 1).

### Antitumor activity of hertuzumab-vcMMAE on NCI-N87 xenografts in nude mice

To evaluate the efficacy of hertuzumab-vcMMAE *in vivo*, we first established NCI-N87 xenografts in nude mice and then

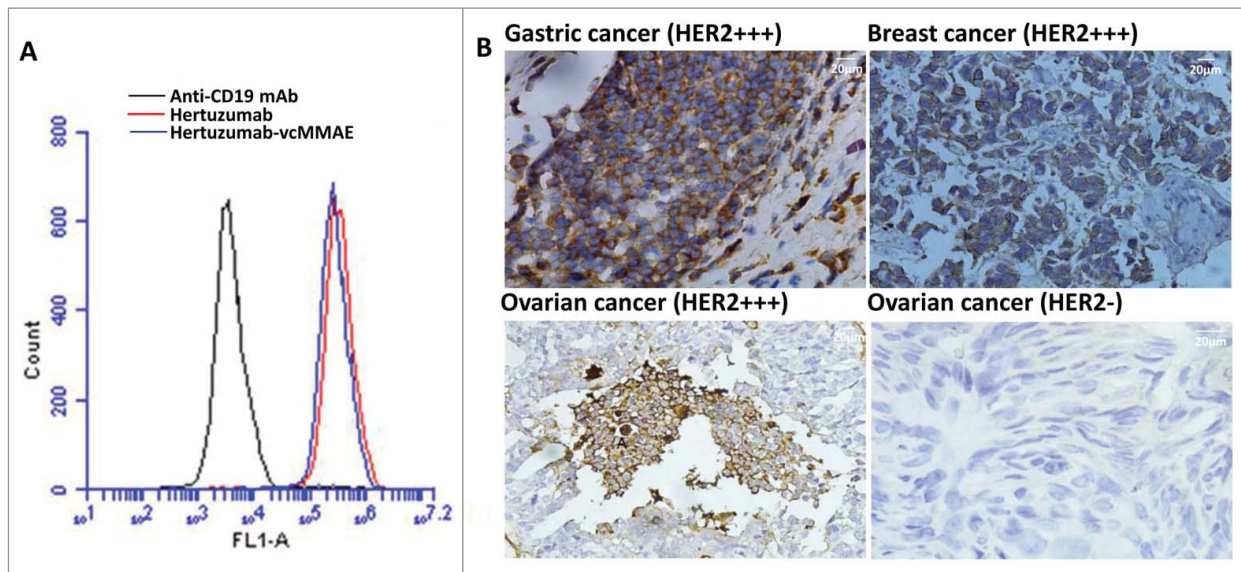


**Figure 2.** Effects of MMAE conjugation on hertuzumab binding to HER2. (A) Flow cytometric assay. Binding of hertuzumab-MMAE and hertuzumab to HER2-positive human gastric cancer cells. NCI-N87 cells were incubated with hertuzumab (Red) and hertuzumab-MMAE (Blue). Anti-CD19 mAb was used as a negative control. Cell membrane bound antibodies or ADCs were detected using FITC labeled anti human IgG by flow cytometry. (B) Immunohistochemistry. Binding specificity of hertuzumab-MMAE for tissue sections. HER2 overexpressing gastric cancer, breast cancer, ovarian cancer and HER2 negative ovarian cancer tissue sections were collected from patients and subjected to immunohistochemical staining with hertuzumab-MMAE. The HER2-positive tumor samples showed an intense staining and no immunoreactions occurred in HER2-negative ones. HER2 status of each section was confirmed by our pathology department.

treated these BALB/c mice with hertuzumab, trastuzumab, hertuzumab-vcMMAE, MMAE and Lapatinib. As shown in Fig. 6 and Table 2, a single intravenous injection of hertuzumab-vcMMAE at doses of 2.5, 5, and 10 mg/kg on day 0 resulted in significant and sustained antitumor effects. The tumor inhibition rate was increased to 133%, 193% and 200%, respectively. In the group administered 2.5 mg/kg, obvious tumor shrinkage was observed in all 6 mice. Tumors disappeared in 5 mice (5/6) in the group receiving 5 mg/kg. At 10 mg/kg group, tumors completely disappeared in all mice (6/6) by day 13. There was no tumor recurrence observed in all hertuzumab treated mice. In contrast, mice treated with 10 mg/kg trastuzumab on days 0, 7, and 14 (delivered a double dose on day 0) showed limited efficacy, with a 49% tumor inhibition rate. Daily administration

of 200 mg/kg Lapatinib from day 0 to day 20 also showed an antitumor effect, with a 78% tumor inhibition rate.

On the second study, mice with NCI-N87 xenografts were treated with an intravenous dose of hertuzumab-vcMMAE on days 0 and 7. The results showed that 0.5 mg/kg hertuzumab-vcMMAE was not sufficient to inhibit tumor growth. However, all tumors in the 5 mg/kg hertuzumab-vcMMAE treated mice disappeared completely. In contrast, the 5 mg/kg hertuzumab and 0.1 mg/kg MMAE mono-treatment and co-treatment groups had poor inhibitory effects on tumor growth. The tumor inhibition rate for hertuzumab and MMAE co-treatment was 15% lower than each mono-treatment.

Body weight was not significantly different between experimental and control groups, suggesting that the different dosing of hertuzumab-vcMMAE, hertuzumab, trastuzumab, MMAE and Lapatinib were all well tolerated.

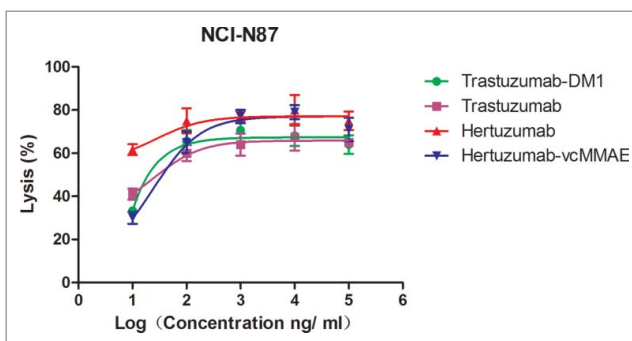


**Figure 3.** ADCC effects of trastuzumab, trastuzumab-DM1, hertuzumab and hertuzumab-MMAE on HER2-positive human gastric cancer NCI-N87 cells. NCI-N87 cells were exposed to a series of concentrations (10, 100, 1,000, 10,000, and 100,000 ng/ml) of antibodies or ADCs followed by incubation with PBMC cells. The lysis rates of NCI-N87 cells for each well were then calculated. Statistical analysis was performed using software GraphPad Prism 5 by nonlinear fit model (log(agonist) vs. response). The results are represented as mean  $\pm$  SD from triplicate experiments.

## Discussion

Targeted therapy against human cancer utilizing specific antibodies conjugated with a chemotherapeutic agent or toxin has become one of the leading novel strategies in cancer therapy.<sup>38</sup> In the current study, we evaluated the efficacy of hertuzumab-vcMMAE on HER2-positive gastric cancer *in vitro* and in a mouse tumor xenograft model. We conjugated hertuzumab to MMAE *via* a Maleimidocaproyl-Valine-Citrulline- p-amino-benzylalcohol-p-Nitrophenyl carbonate linker and then assayed its effects on HER2-positive and negative gastric cancer cells *in vitro* and in nude mice in comparison to hertuzumab, trastuzumab, MMAE, and Lapatinib. Our data showed that hertuzumab-vcMMAE maintained HER2 binding but had enhanced antitumor activity in HER2-positive gastric cancer cells *in vitro* and in nude mice. Our data were consistent with a previous study showing that trastuzumab-DM1 possessed a significant



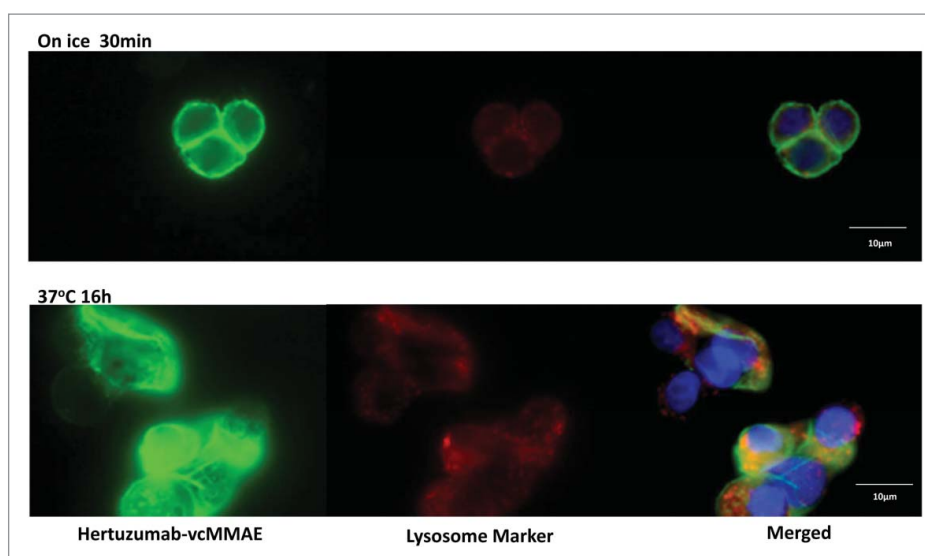


**Figure 4.** Internalization and trafficking of hertuzumab-MMAE to the lysosome in NCI-N87 cells. N87 cells were incubated with hertuzumab-MMAE on ice or 37°C. Hertuzumab-MMAE was detected using Alexa Fluor 488-labeled goat antihuman IgG and are shown in green. Lysosomes were visualized using a mouse anti-human Lamp-2 antibody followed by Alexa-Fluor® 647 labeled goat anti-mouse IgG and are shown in red. DAPI-stained nuclei are in blue. The orange signal in the merged image represents the hertuzumab-MMAE in the lysosome

antitumor effect in HER2-positive gastric cancer pre-clinically,<sup>39</sup> which led to 2 clinical trials undergoing safety and efficacy examination of trastuzumab-DM1 in patients with HER2 positive gastric cancer.<sup>40,41</sup>

In our current study, we utilized a humanized anti-HER2 monoclonal antibody, hertuzumab, that we generated by screening HER2-specific murine monoclonal antibodies to human HER2 antigen. Hertuzumab-derived ADC was generated by conjugating it to MMAE *via* the Valine-Citrulline (VC) linker. The antigen binding site is an intrinsic characteristic of therapeutic antibodies and the basis for conjugation with chemotherapeutic agents or drugs.<sup>22,42</sup> In the current study, we found that the hertuzumab targeted epitope was distinct from the epitope recognized by trastuzumab. We also found the affinity between HER2 and hertuzumab was higher than that of trastuzumab. Furthermore, the ADCC effect of naked hertuzumab was nearly 2-fold stronger compared to trastuzumab *in vitro*. The ADCC effect is a main mechanism for tumor-killing by the naked antibody. According to a previous study, deficiency in the ADCC effect of trastuzumab in breast cancer

patients was directly associated with trastuzumab resistance.<sup>43</sup> All these data indicate that hertuzumab is an anti-HER2 antibody with high affinity and effective functions.

Our current data further showed that after conjugation with MMAE, the binding activity of hertuzumab to HER2-positive gastric cancer cells was not dramatically altered. The binding specificity of hertuzumab-vcMMAE was also confirmed in HER2-positive clinical tumor tissue samples. The decrease in hertuzumab mediated ADCC effect after conjugation with MMAE is consistent with a previous study.<sup>31</sup> Moreover, the conformational change of the Fc region of the conjugated antibody maybe associated with this phenomenon. Although the ADCC effect was decreased, the overall cytotoxicity against HER2-positive gastric cancer cells by hertuzumab-vcMMAE was significantly increased due to the fact that the ADC drug is enhanced by conjugated cytotoxin MMAE. Indeed, our *in vitro* assay showed that hertuzumab-vcMMAE had a much stronger antitumor effect in NCI-N87 cells compared to trastuzumab-DM1. This may be due to 2 reasons. First, hertuzumab has a higher affinity to HER2

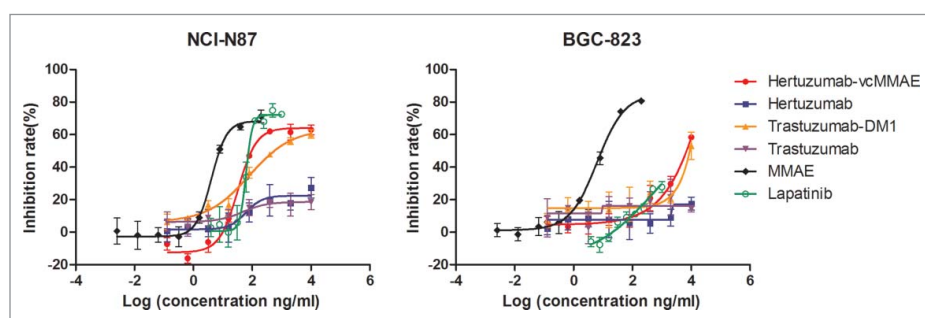


**Figure 5.** Antitumor activity of Abs, ADCs and small molecule drugs in gastric cancer cells *in vitro*. The anti-proliferative effect of hertuzumab, hertuzumab-MMAE, trastuzumab, and trastuzumab-DM1 was assessed at concentrations of 0.128, 0.64, 3.2, 16, 80, 400, 2,000, and 10,000 ng/ml in gastric cancer NCI-N87 and BGC-823 cells *in vitro*. The effect of free MMAE was tested at concentrations of 0.00256, 0.0128, 0.064, 0.32, 1.6, 8, 40, and 200 ng/ml. The effect of Lapatinib was tested at concentrations of 3.9, 7.8, 15.625, 31.25, 62.5, 125, 250, 500, and 1,000 ng/ml. The data are summarized as mean  $\pm$  SD from triplicate experiments

**Table 1.** Cytotoxicity of Abs, ADCs and small molecule drugs on HER2-positive and negative gastric cancer cells *in vitro*.

Cell line	HER2 status	IC50 (ng/ml)						
		Hertuzumab-vcMMAEs		Free MMAE	Hertuzumab	Trastuzumab- DM1	Trastuzumab	Lapatinib
		Hertuzumab-vcMMAE	Conjugated MMAE					
NCI-N87	HER2+	95.3	1.9	7.7	>10000	568.2	>10000	75.6
BGC-823	HER2-	6927.3	138.5	9.1	>10000	8904.8	>10000	>1000

than trastuzuman-DM1. Secondly, MMAE conjugated through the VC linker is optimal compared to DM1 conjugation. We also observed that treatment of NCI-N87 tumor cells with hertuzumab or trastuzumab individually showed relatively poor inhibition of cell growth, which is similar to the published data.<sup>39</sup> Furthermore, both hertuzumab and hertuzumab-vcMMAE had a poor or non-inhibitory effect on HER2-negative gastric cancer cells, suggesting that a highly selective HER2 molecule on the cancer cell membrane is necessary to mediate the effects of hertuzumab-vcMMAE. Our current study was further confirmed by the *in vivo* experiments with hertuzumab-vcMMAE. We showed highly potent and sustained tumor inhibition activity of hertuzumab-vcMMAE in NCI-N87 xenografts at a relatively low dose. Compared to hertuzumab-vcMMAE, the equivalent hertuzumab and MMAE co-treatment was insufficient to inhibit tumor growth *in vivo*. This finding suggests that conjugation of hertuzumab with MMAE greatly increased the efficacy of MMAE antitumor activity.

In conclusion, our current study of hertuzumab-vcMMAE anti-tumor activity *in vitro* and *in vivo* indicates that hertuzumab-vcMMAE is a highly effective novel therapy to target HER2-positive gastric cancer. Future studies will investigate bioavailability and clinical safety before administering this treatment to patients.

## Materials and methods

### Reagents

Trastuzumab and trastuzumab-DM1 was purchased from Hoffman-La Roche Ltd (Basel, Switzerland). DAPI (4',6-diamidino-2-phenylindole) was purchased from Roche diagnostics GmbH (Mannheim, Germany). Cytofix/Cytoperm™ Kit was from BD biosciences (San Diego, CA, USA). A mouse anti-human Lamp-2 and goat anti-mouse IgG Alexa-Fluor® 647 were purchased from Abcam (Cambridge, MA, USA). A goat anti-human IgG Alexa-Fluor® 488 and

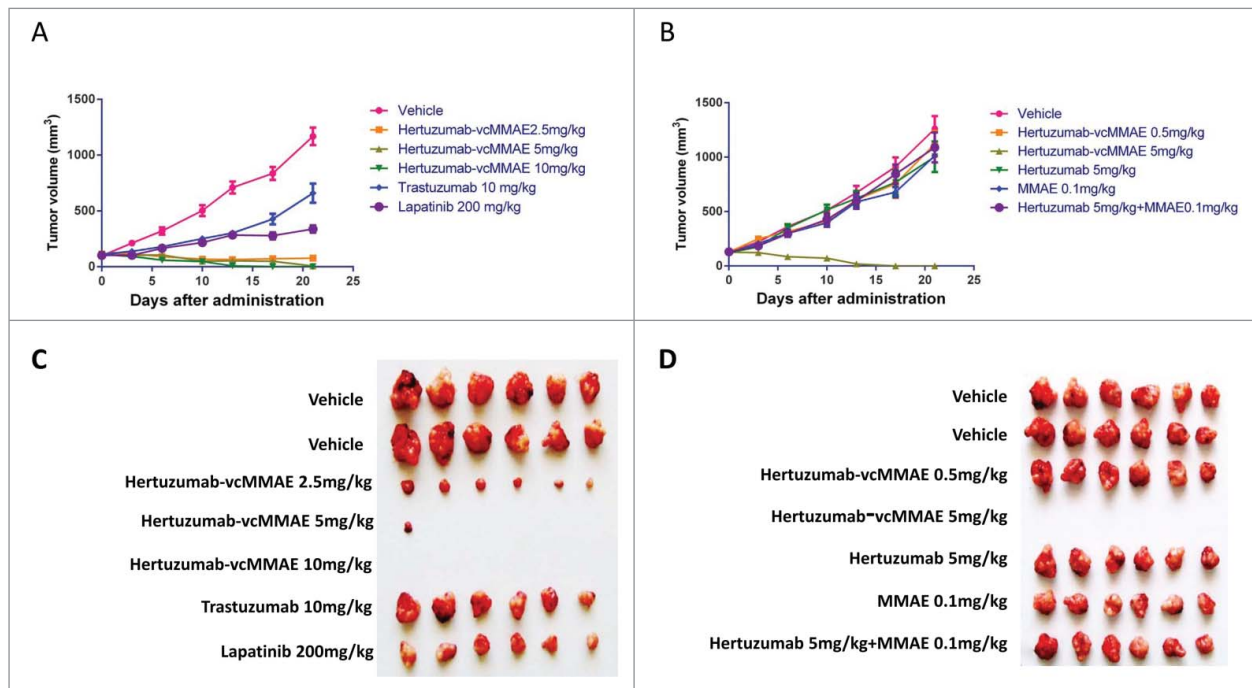


**Figure 6.** *In vivo* antitumor activity of Abs, ADC and small molecule drugs in NCI-N87 xenograft models. (A) *In vivo* tumor inhibition effect of the first run treatment. Hertuzumab-MMAE was given as a single intravenous injection at doses of 2.5, 5 or 10 mg/kg on day 0. Herceptin (10 mg/kg) was injected intravenously on days 0, 7, and 14. Lapatinib (200 mg/kg) was given daily through intragastric administration from day 0 to day 20. (B) *In vivo* tumor inhibition effect of the second run treatment. The effects of hertuzumab-vcMMAE (0.5 or 5 mg/kg), hertuzumab (5 mg/kg), free MMAE (0.1 mg/kg equivalent of 5 mg/kg hertuzumab-vcMMAE) mono-treatment, and hertuzumab at 5 mg/kg, MMAE at 0.1 mg/kg co-treatment were evaluated. The mice in all groups were administrated drug at days 0 and 7 after randomization. (C) Subcutaneous tumors in the first run treatment were measured at day 21. (D) Subcutaneous tumors in the second run treatment were measured at day 21

**Table 2.** Antitumor effect of Abs, ADC and small molecule drugs on HER2 positive gastric cancer NCI-N87 cell xenografts.

Groups	Route of administration and frequency	Mean tumor volume $\pm$ SD (mm <sup>3</sup> )		Tumor inhibition rate (%)	P value*	Observed tumor size on Day21
		D0	D21			
Vehicle	iv, D0	98.2 $\pm$ 10.3	1167.7 $\pm$ 272.8	—	—	
Hertuzumab-vcMMAE2.5 mg/kg	iv, D0	114.9 $\pm$ 12.7	76.9 $\pm$ 25.4	133	abc	6/6 PR
Hertuzumab-vcMMAE 5 mg/kg	iv, D0	107.4 $\pm$ 11.7	7.4 $\pm$ 18.2	193	abc	1/6 PR, 5/6 CR
Hertuzumab-vcMMAE10 mg/kg	iv, D0	109.0 $\pm$ 22.0	0.0 $\pm$ 0.0	200	abc	6/6 CR
Trastuzumab 10 mg/kg	iv, D0, 7, 14	112.3 $\pm$ 12.0	658.8 $\pm$ 210.4	49	a	
Lapatinib 200 mg/kg	po, D0-20	102.4 $\pm$ 4.7	338.3 $\pm$ 79.7	78	a	
Vehicle	iv, D0, 7	127.2 $\pm$ 15.7	1260.5 $\pm$ 404.6	—	—	
Hertuzumab-vcMMAE0.5 mg/kg	iv, D0, 7	128.0 $\pm$ 16.7	1122.3 $\pm$ 289.5	12	—	
Hertuzumab-vcMMAE5 mg/kg	iv, D0, 7	126.4 $\pm$ 26.6	0.0 $\pm$ 0.0	200	ad	6/6 CR
Hertuzumab5 mg/kg	iv, D0, 7	122.3 $\pm$ 9.2	1004.0 $\pm$ 344.4	22	—	
MMAE 0.1 mg/kg	iv, D0, 7	121.7 $\pm$ 20.1	1013.2 $\pm$ 150.5	21	—	
Hertuzumab 5 mg/kg + MMAE 0.1 mg/kg.	iv, D0, 7	131.2 $\pm$ 11.7	1089.4 $\pm$ 337.9	15	—	

D0 Days after random grouping

iv intravenous injection

Po intragastric administration

PR Tumor size was reduced compared to the vehicle group, but still observed

CR Tumors vanished completely

<sup>a</sup> $P < 0.001$  vs. Vehicle<sup>b</sup> $P < 0.001$  vs. Trastuzumab<sup>c</sup> $P < 0.001$  vs. Lapatinib<sup>d</sup> $P < 0.001$  vs. Hertuzumab 5 mg/kg + MMAE 0.1 mg/kg\* Student's *t* test.

Calcein-AM were purchased from Invitrogen (Carlsbad, CA, USA). A FITC labeled goat anti-human IgG Fc was from BETHYL laboratories (Montgomery, TX, USA). Lapatinib was obtained from GlaxoSmithKline (GSK, Middlesex, UK). vcMMAE was purchased from Concertis Biosystems, Corp (San Diego, CA, USA). The CCK-8 kit was from Dojindo Lab (Kumamoto, Japan). The SABC-POD kit was obtained from BOSTER (Wuhan, China). The biotinylated human HER2 protein extracellular domain (HER2-ECD) was purchased from G&P bioscience (Santa Clara, CA, USA) and Streptavidin (SA) biosensors were purchased from Fortibio (Menlo Park, CA, USA). Diethylenetriaminepentaacetic acid (DTPA) was from Aldrich (Milwaukee, WI, USA).

### Cell lines and culture

HER2-positive human gastric cancer cell line NCI-N87 was obtained from American Type Culture Collection (ATCC, Manassas, VA, USA) and HER2-negative human gastric cancer BGC-823 cell line was from Simcere (Yantai, China). These cell lines were cultured in RM1640 medium supplemented with 10% fetal bovine serum (FBS) in a humidified incubator with 5% CO<sub>2</sub> at 37°C.

### Preparation of hertuzumab

Hertuzumab expressed CHO cell line (DG44 derived) was seeded in a STR50L bioreactor (Sartorius Stedim, Guxhagen, Germany) and we performed feed batch cultivation. Hertuzumab was then purified using Protein A affinity chromatography and Sepharose High Performance chromatography. The purity of hertuzumab was analyzed by sodium dodecyl sulfate-polyacrylamide electrophoresis (SDS-PAGE) and the concentration was determined by UV absorption at 280 nm.

### Conjugation of hertuzumab-vcMMAE

10 mg/ml of hertuzumab was mixed with 0.15 mM Tris (2-chloroethyl) phosphate (TCEP) and 1 mM DTPA at 25°C for 2 h and then incubated at 10°C for 1 h. After that, one portion of 0.8 mM vcMMAE dissolved in dimethyl sulfoxide (DMSO) was added into 3 portions of reduced antibody solution, mixed, and then incubated at 25°C for 1 h. The ADC was then purified using a pre-equilibrated Sephadex G25 column and ADC concentration was determined by UV absorption at 280 nm and the drug/Ab ratio was determined by hydrophobic interaction chromatography-high performance liquid chromatography (HIC-HPLC).

### The Octet assay to detect the binding capacity of hertuzumab-vcMMAE to HER2-ECD

Octet QK (Forte-bio) was used to assess the Ag-Ab binding characteristics. Octet assay harnesses biolayer interferometry to detect and quantify molecular interactions.<sup>44</sup> In brief, the sample plate was agitated at 600 rpm and the prewet SA sensors were dipped into 10  $\mu$ g/ml biotinylated HER2-ECD for 15 min. After equilibration in phosphate buffered saline (PBS) for 3 min, the HER2-ECD coated sensors were dipped into 50  $\mu$ g/ml hertuzumab, hertuzumab-vcMMAE, and trastuzumab containing wells of the microplate for 15 min. The hertuzumab, hertuzumab-vcMMAE and trastuzumab saturated sensors were then dipped into PBS for 30 min to determine their dissociation parameters, respectively. Moreover, to identify the antibody binding epitope of hertuzumab and trastuzumab, the hertuzumab and trastuzumab saturated sensors were equilibrated in PBS for 3 min and then dipped into 50  $\mu$ g/ml trastuzumab and hertuzumab solution, respectively for 15 min. The dissociation was performed in PBS for 30 min. The real time biolayer shift value was recorded and the affinity constant ( $K_D$ ) was

calculated applying a 1:1 interaction model by Octet software (version 3.1, Forte-bio, Menlo Park, CA, USA).

### Flow cytometry assay

NCI-N87 cells were trypsinized in 0.25% trypsin in PBS (pH7.4) and centrifuged at 1000 rpm for 5 min and the cell pellets were resuspended in 50  $\mu$ l PBS (pH7.4) supplemented with 1% bovine serum albumin (BSA). Cell density was adjusted to  $6 \times 10^6$  cells/ml and incubated with 40  $\mu$ g/ml hertuzumab or hertuzumab-vcMMAE for 30 min at 4°C. After being washed twice with PBS, the cells were further incubated with 10  $\mu$ g/ml FITC labeled goat anti-human IgG Fc for 30 min at 4°C and then washed twice with PBS and fixed in 1% paraformaldehyde. The fluorescence intensity of FITC was measured using an Accuri<sup>TM</sup> flow cytometer (BD biosciences, San Jose, CA, USA). The purified human IgG obtained from healthy human serum was used as a negative control.

### Immunohistochemistry

Tumor tissue sections were obtained from the pathology department of Yuhuangding Hospital (Yantai, China). HER2 expression in gastric cancer tissues was detected using the SABC-POD kit following the manufacture's instructions. Briefly, after dewaxing in xylene, the sections were subjected to antigen retrieval in a citrate buffer (pH6.0) at 99°C for 20 min in a microwave and then subjected to incubation with rabbit serum. The sections were further incubated with hertuzumab-vcMMAE at 37°C for 1 h and with the biotin labeled goat anti-human IgG, the secondary antibody. The bound hertuzumab-vcMMAE was visualized by SBA (streptavidin-biotin-peroxidase complex) and diaminobenzidine. Sections were counterstained with hematoxylin and eosin (H&E) and mounted with a covers lip. The sections were viewed and scored under a microscope at a magnification of 40X.

### Antibody-dependent cell-mediated cytotoxicity (ADCC) assay

HER2-positive gastric cancer NCI-N87 cells were incubated with Calcein-AM for 20 min at 37°C and then seeded into 96 well plates at a density of  $1 \times 10^4$  cells/well in triplicate. Different concentrations of hertuzumab, hertuzumab-vcMMAE, trastuzumab, and trastuzumab-DM1 (10 ng, 100 ng, 1  $\mu$ g, 10  $\mu$ g, and 100  $\mu$ g/mL) were added into each well of the cell culture plates for spontaneous and maximum release of calcein. After incubation for 1 h, the cells were exposed to human peripheral blood mononuclear cells (PBMC) at a density of  $2.5 \times 10^4$  cells/well for 4 h. Triplicate wells without antibodies and ADCs were used as blank controls. Triplicate wells with hertuzumab-vcMMAE or trastuzumab-DM1, but without PBMC, were used as an ADC control. The cultured medium was centrifuged and the supernatant was collected to examine the fluorescence value (F, sample, F<sub>i</sub>, blank control and F<sub>i</sub>', ADC control). The cultured medium without centrifugation was lysed using 2% Triton X-100 and the total fluorescence value (F<sub>t</sub>) was measured using the SpectraMax M2e microplate reader (Molecular Devices, Sunnyvale, CA, USA) with excitation at 490 nm and

emission at 515 nm. Cell lysis rate (R<sub>l</sub>) of the antibodies was calculated using the formula  $R_l = (F - F_i)/F_t \times 100\%$ . Cell lysis rate (R<sub>l</sub>) of ADCs was calculated using the formula  $R_l = (F - F_i - F_i')/F_t \times 100\%$ .

### Hertuzumab-vcMMAE trafficking assay

Hertuzumab-vcMMAE lysosomal trafficking was examined according to a published method.<sup>45</sup> Briefly, NCI-N87 cells were trypsinized and seeded on a Labtek<sup>®</sup> glass chamber slider (Thermo Scientific, Waltham, MA, USA) at a density of 10,000 cells/well. After incubation for 18 h at 37°C, the cells were further incubated with 5  $\mu$ g/ml hertuzumab-vcMMAE for 30 min on ice or for 16 h at 37°C. The cells were washed twice with cold PBS to remove unbound ADCs and then exposed to Cytofix/cytoperm reagent (200  $\mu$ l/well) for 25 min at 4°C. After being washed twice with 1X perm/wash buffer, lysosomal compartments were bound by a mouse anti-human Lamp-2 antibody and then detected by Alexa-Fluor<sup>®</sup> 647 labeled goat anti-mouse IgG. Hertuzumab-ADC was visualized by staining with Alexa Fluor 488-labeled goat anti-human IgG. Nuclear compartments were stained with DAPI. Fluorescence was visualized with a microscope (Nikon, Japan).

### In vitro cell cytotoxicity assay

Cells were trypsinized and seeded at a density of  $1 \times 10^5$  cells/well in 96 well tissue culture plates (Greiner, Nürtingen, Germany). The cytotoxicity of hertuzumab, hertuzumab-MMAE, trastuzumab, and trastuzumab-DM1 was evaluated at concentrations of 0.128, 0.64, 3.2, 16, 80, 400, 2,000, and 10,000 ng/ml in gastric cancer NCI-N87 and BGC-823 cells *in vitro*. The effect of free MMAE was measured at concentrations of 0.00256, 0.0128, 0.064, 0.32, 1.6, 8, 40, and 200 ng/ml as a control. The effect of Lapatinib was assayed at concentrations 3.9, 7.8, 15.625, 31.25, 62.5, 125, 250, 500, and 1,000 ng/ml. The cells were cultured with these agents for 72 h and 10  $\mu$ l/well of CCK-8 reagent was added into each well. The absorbent Optical Density (OD) value at 450 nm was measured using a SpectraMax M2e microplate reader. The OD values of samples were normalized to values of the blank well with just cell culture media without cells.

### Nude mouse xenograft assay

Female BALB/cA-nude mice aged 6 to 7 weeks were obtained from SLCA laboratory animal Ltd (Shanghai, China). The animals were acclimated for one week prior to experimentation. The mice were housed in a temperature and humidity controlled environment with a controlled light-dark cycle (12 h–12 h). During the animal experiments, the BALB/cA-nude mice were injected subcutaneously with  $7 \times 10^6$  NCI-N87 cells. The treatment was started when the tumor volume reached 100–200 mm.<sup>3</sup> The mice were randomized into 2 groups and 2 different experiments were performed to confirm the efficacy of hertuzumab-vcMMAE on NCI-N87 xenografts. The dosing strategy of the first experiment was performed as follows. Hertuzumab-vcMMAE was given as a single intravenous injection at a dose of 2.5, 5 or 10 mg/kg on day 0. Trastuzumab



(10 mg/kg) was injected intravenously on days 0, 7 and 14. Lapatinib (200 mg/kg) was given daily through intragastric administration from day 0 to day 20. For the second experiment, hertuzumab-vcMMAE was given intravenously at day 0 and 7 at a dose of 0.5 and 5 mg/kg, respectively. Hertuzumab (5 mg/kg) was injected intravenously on days 0 and 7. MMAE (0.1 mg/kg) was given intravenously on days 0 and 7. PBS (pH7.4) was injected intravenously at the same volume as a control for each experiment. Tumor diameters were measured with a caliper and tumor volume was calculated using the formula:  $T_{vol}=(A \times B^2)/2$ ; where A is the larger diameter of the tumor and B is the smaller diameter perpendicular to A. Tumor inhibition rate ( $R_i$ ) was calculated using the formula:  $R_i = (1-(T-T_0)/(C-C_0)) \times 100\%$ . When the tumor subsided at the end of the treatment  $R_i = (1-(T-T_0)/T_0) \times 100\%$ . T and C are the tumor volume at the end of the treatment of experimental and control groups, respectively.  $T_0$  and  $C_0$  represent the tumor volume at the beginning of the experimental and control groups, respectively. Animals were euthanized by CO<sub>2</sub> inhalation at the end of experiments.

### Disclosure of potential conflicts of interest

Hongwen Li, Jing Jiang, Changjiang Huang, Xuejing Yao, Qiaoyu Xu, Fang Yu, Chao Yu and Jianmin Fang are stock holders of RemeGen, Ltd. All others authors declared no conflicts of interest in this work.

### Funding

This work was supported in part by grants from National Science and Technology Major Project of China (#2014ZX09508004001 and #2013ZX09401002), National Basic Research of China 973 program (#2015cb553706), and National Natural Science Foundation of China (#31270987).

### References

- Karimi P, Islami F, Anandasabapathy S, Freedman ND, Kamangar F. Gastric Cancer: Descriptive Epidemiology, Risk Factors, Screening, and Prevention. *Cancer Epidem Biomar* 2014; 23:700-13; PMID:24618998; <http://dx.doi.org/10.1158/1055-9965.EPI-13-1057>
- Siegel R, Ma J, Zou Z, Jemal A. *Cancer statistics, 2014*. *CA* 2014; 64:9-29; PMID:24399786; <http://dx.doi.org/10.1017/S0009840X13002084>
- Shimoyama S. Unraveling trastuzumab and lapatinib inefficiency in gastric cancer: Future steps (Review). *Mol Clin Oncol* 2014; 2:175-81; PMID:24649329; <http://dx.doi.org/10.3892/mco.2013.218>
- Weinstein IB, Joe AK. Mechanisms of disease: Oncogene addiction—a rationale for molecular targeting in cancer therapy. *Nat Clin Pract Oncol* 2006; 3:448-57; PMID:16894390; <http://dx.doi.org/10.1038/nponc0558>
- Yan M, Parker BA, Schwab R, Kurzrock R. HER2 aberrations in cancer: implications for therapy. *Cancer Treat Rev* 2014; 40:770-80; PMID:24656976; <http://dx.doi.org/10.1016/j.ctrv.2014.02.008>
- Gao N, Xu H, Liu C, Xu H, Chen G, Wang X, Li Y, Wang Y. Nestin: predicting specific survival factors for breast cancer. *Tumour Biol* 2014; 35:1751-5; PMID:24443256; <http://dx.doi.org/10.1007/s13277-013-1548-7>
- Marmor MD, Skaria KB, Yarden Y. Signal transduction and oncogenesis by ErbB/HER receptors. *Int J Radiat Oncol Biol Phys* 2004; 58:903-13; PMID:14967450; <http://dx.doi.org/10.1016/j.ijrobp.2003.06.002>
- Helikar T, Kochi N, Kowal B, Dimri M, Naramura M, Raja SM, Band V, Band H, Rogers JA. A comprehensive, multi-scale dynamical model of ErbB receptor signal transduction in human mammary epithelial cells. *PLoS One* 2013; 8:e61757; PMID:23637902; <http://dx.doi.org/10.1371/journal.pone.0061757>
- Zhang Y, Opreko L, Shankaran H, Chrisler WB, Wiley HS, Resat H. HER/Erbb receptor interactions and signaling patterns in human mammary epithelial cells. *BMC Cell Biol* 2009; 10:78; PMID:19878579; <http://dx.doi.org/10.1186/1471-2121-10-78>
- Beltran Garate B, Yabar Berrocal A. [HER2 expression in gastric cancer in Peru]. *Rev Gastroenterol Peru* 2010; 30:324-7; PMID:21263759
- Yu GZ, Chen Y, Wang JJ. Overexpression of Grb2/HER2 signaling in Chinese gastric cancer: their relationship with clinicopathological parameters and prognostic significance. *J Cancer Res Clin Oncol* 2009; 135:1331-9; PMID:19337752; <http://dx.doi.org/10.1007/s00432-009-0574-8>
- Zhu Z, Wang J, Sun Z, Sun X, Wang Z, Xu H. Flotillin2 expression correlates with HER2 levels and poor prognosis in gastric cancer. *PLoS One* 2013; 8:e62365; PMID:23658725; <http://dx.doi.org/10.1371/journal.pone.0062365>
- Janjigian YY, Werner D, Pauligk C, Steinmetz K, Kelsen DP, Jager E, Altmannsberger HM, Robinson E, Tafel LJ, Tang LH, et al. Prognosis of metastatic gastric and gastroesophageal junction cancer by HER2 status: a European and USA International collaborative analysis. *Ann Oncol* 2012; 23:2656-62; PMID:2268179; <http://dx.doi.org/10.1093/annonc/mds104>
- Sheng WQ, Huang D, Ying JM, Lu N, Wu HM, Liu YH, Liu JP, Bu H, Zhou XY, Du X. HER2 status in gastric cancers: a retrospective analysis from four Chinese representative clinical centers and assessment of its prognostic significance. *Ann Oncol* 2013; 24:2360-4; PMID:23788757; <http://dx.doi.org/10.1093/annonc/mdt232>
- Graziano C. HER-2 breast assay, linked to Herceptin, wins FDA's okay. *CAP Today* 1998; 12(1), 14-6; PMID:10187049
- Kurokawa Y, Sugimoto N, Miwa H, Tsuda M, Nishina S, Okuda H, Imamura H, Gamoh M, Sakai D, Shimokawa T, et al. Phase II study of trastuzumab in combination with S-1 plus cisplatin in HER2-positive gastric cancer (HERBIS-1). *Br J Cancer* 2014; 110:1163-8; PMID:24473399; <http://dx.doi.org/10.1038/bjc.2014.18>
- Bang YJ, Van Cutsem E, Feyereislova A, Chung HC, Shen L, Sawaki A, Lordick F, Ohtsu A, Omuro Y, Satoh T, et al. Trastuzumab in combination with chemotherapy versus chemotherapy alone for treatment of HER2-positive advanced gastric or gastro-oesophageal junction cancer (ToGA): a phase 3, open-label, randomised controlled trial. *Lancet* 2010; 376:687-97; PMID:20728210; [http://dx.doi.org/10.1016/S0140-6736\(10\)61121-X](http://dx.doi.org/10.1016/S0140-6736(10)61121-X)
- Ding X, Qu X, Fan Y, Che X, Qu J, Xu L, Liu J, Liu Y. Trastuzumab and oxaliplatin exhibit a synergistic antitumor effect in HER2-positive gastric cancer cells. *Anti-Cancer Drug* 2014; 25:315-22; PMID:24300914; <http://dx.doi.org/10.1097/CAD.0000000000000048>
- Shiraishi K, Mimura K, Izawa S, Inoue A, Shiba S, Maruyama T, Watanabe M, Kawaguchi Y, Inoue M, Fujii H, et al. Lapatinib acts on gastric cancer through both antiproliferative function and augmentation of trastuzumab-mediated antibody-dependent cellular cytotoxicity. *Gast Cancer* 2013; 16:571-80; PMID:23187882; <http://dx.doi.org/10.1007/s10120-012-0219-5>
- Sakai D, Satoh T, Kurokawa Y, Kudo T, Nishikawa K, Oka Y, Tsujinaka T, Shimokawa T, Doki Y, Furukawa H. A phase II trial of trastuzumab combined with irinotecan in patients with advanced HER2-positive chemo-refractory gastric cancer: Osaka Gastrointestinal Cancer Chemotherapy Study Group OGS1203 (HERBIS-5). *Jpn J Clin Oncol* 2013; 43:838-40; PMID:23852648; <http://dx.doi.org/10.1093/jjco/hyt083>
- Dai GH, Shi Y, Chen L, Lv YL, Zhong M. Trastuzumab combined with docetaxel-based regimens in previously treated metastatic gastric cancer patients with HER2 over-expression. *Hepato-Gastroenterol* 2012; 59:2439-44; PMID:22534547; <http://dx.doi.org/10.5754/hge12166>
- Ko BK, Lee SY, Lee YH, Hwang IS, Persson H, Rockberg J, Borrebaeck C, Park D, Kim KT, Uhlen M, et al. Combination of novel HER2-targeting antibody 1E11 with trastuzumab shows synergistic antitumor activity in HER2-positive gastric cancer. *Mol Oncol* 2014; PMID:25306393; <http://dx.doi.org/10.1016/j.molonc.2014.09.007>
- Tanner M, Kapanen AI, Junttila T, Raheem O, Grenman S, Elo J, Elenius K, Isola J. Characterization of a novel cell line established



- from a patient with Herceptin-resistant breast cancer. *Mol Cancer Therapeut* 2004; 3:1585-92; PMID:15634652
24. Chan CT, Metz MZ, Kane SE. Differential sensitivities of trastuzumab (Herceptin)-resistant human breast cancer cells to phosphoinositide-3 kinase (PI-3K) and epidermal growth factor receptor (EGFR) kinase inhibitors. *Breast Cancer Res Treat* 2005; 91:187-201; PMID:15868447; <http://dx.doi.org/10.1007/s10549-004-7715-1>
  25. Panowski S, Bhakta S, Raab H, Polakis P, Junutula JR. Site-specific antibody drug conjugates for cancer therapy. *mAbs* 2014; 6:34-45; PMID:24423619; <http://dx.doi.org/10.4161/mabs.27022>
  26. Loke J, Khan JN, Wilson JS, Craddock C, Wheatley K. Mylotarg has potent anti-leukaemic effect: a systematic review and meta-analysis of anti-CD33 antibody treatment in acute myeloid leukaemia. *Ann Hematol* 2015; 94:361-73; PMID:25284166; <http://dx.doi.org/10.1007/s00277-014-2218-6>
  27. FDA approves brentuximab vedotin for Hodgkin lymphoma and systemic anaplastic large-cell lymphoma. *Oncology (Williston Park)* 2011; 25:904; PMID:22010386
  28. Ballantyne A, Dhillon S. Trastuzumab emtansine: first global approval. *Drugs* 2013; 73:755-65; PMID:23620199; <http://dx.doi.org/10.1007/s40265-013-0050-2>
  29. Mullard A. Maturing antibody-drug conjugate pipeline hits 30. *Nat Rev Drug Discov* 2013; 12:329-33; PMID:23629491; <http://dx.doi.org/10.1038/nrd4009>
  30. Ma D, Hopf CE, Malewicz AD, Donovan GP, Senter PD, Goeckeler WF, Maddon PJ, Olson WC. Potent antitumor activity of an auristatin-conjugated, fully human monoclonal antibody to prostate-specific membrane antigen. *Clin Cancer Res* 2006; 12:2591-6; PMID:16638870; <http://dx.doi.org/10.1158/1078-0432.CCR-05-2107>
  31. Li ZH, Zhang Q, Wang HB, Zhang YN, Ding D, Pan LQ, Miao D, Xu S, Zhang C, Luo PH, et al. Preclinical studies of targeted therapies for CD20-positive B lymphoid malignancies by Ofatumumab conjugated with auristatin. *Invest New Drug* 2014; 32:75-86; PMID:23903896; <http://dx.doi.org/10.1007/s10637-013-9995-y>
  32. Gerber HP, Kung-Sutherland M, Stone I, Morris-Tilden C, Miyamoto J, McCormick R, Alley SC, Okeley N, Hayes B, Hernandez-Ilizaliturri FJ, et al. Potent antitumor activity of the anti-CD19 auristatin antibody drug conjugate hBU12-vcMMAE against rituximab-sensitive and -resistant lymphomas. *Blood* 2009; 113:4352-61; PMID:19147785; <http://dx.doi.org/10.1182/blood-2008-09-179143>
  33. Dornan D, Bennett F, Chen Y, Dennis M, Eaton D, Elkins K, French D, Go MA, Jack A, Junutula JR, et al. Therapeutic potential of an anti-CD79b antibody-drug conjugate, anti-CD79b-vc-MMAE, for the treatment of non-Hodgkin lymphoma. *Blood* 2009; 114:2721-9; PMID:19633198; <http://dx.doi.org/10.1182/blood-2009-02-205500>
  34. Afar DE, Bhaskar V, Ibsen E, Breinberg D, Henshall SM, Kench JG, Drobnjak M, Powers M, Wong M, Evangelista F, et al. Preclinical validation of anti-TMEFF2-auristatin E-conjugated antibodies in the treatment of prostate cancer. *Mol Cancer Therapeut* 2004; 3:921-32; PMID:15299075
  35. DiPippo VA, Olson WC, Nguyen HM, Brown LG, Vessella RL, Corey E. Efficacy studies of an antibody-drug conjugate PSMA-ADC in patient-derived prostate cancer xenografts. *The Prostate* 2015; 75:303-13; PMID: 25327986; <http://dx.doi.org/10.1002/pros.22916>
  36. Scales SJ, Gupta N, Pacheco G, Firestein R, French DM, Koeppen H, Rangell L, Barry-Hamilton V, Luis E, Chuh J, et al. An antimesothelin-monomethyl auristatin e conjugate with potent antitumor activity in ovarian, pancreatic, and mesothelioma models. *Mol Cancer Therapeut* 2014; 13:2630-40; PMID:25249555; <http://dx.doi.org/10.1158/1535-7163.MCT-14-0487-T>
  37. Yao X, Jiang J, Wang X, Huang C, Li D, Xie K, Xu Q, Li H, Li Z, Lou L, et al. A novel humanized anti-HER2 antibody conjugated with MMAE exerts potent anti-tumor activity. *Breast Cancer Res Treat* 2015; 153:123-33; PMID:26253944; <http://dx.doi.org/10.1007/s10549-015-3503-3>
  38. Okeley NM, Alley SC, Senter PD. Advancing antibody drug conjugation: from the laboratory to a clinically approved anticancer drug. *Hematol Oncol Clin North America* 2014; 28:13-25; PMID:24287064; <http://dx.doi.org/10.1016/j.hoc.2013.10.009>
  39. Barok M, Tanner M, Koninki K, Isola J. Trastuzumab-DM1 is highly effective in preclinical models of HER2-positive gastric cancer. *Cancer Lett* 2011; 306:171-9; PMID:21458915; <http://dx.doi.org/10.1016/j.canlet.2011.03.002>
  40. Roche H-L. A study of trastuzumab emtansine versus taxane in patients with advanced gastric Cancer 2014.
  41. Roche H-L. A combination study of Kadcyla (Trastuzumab Emtansine) and capecitabine in patients with HER2-Positive metastatic breast cancer and patients with HER2-Positive locally advanced/ metastatic gastric. *Cancer*. 2014.
  42. Lu D, Burris HA, 3rd, Wang B, Dees EC, Cortes J, Joshi A, Gupta M, Yi JH, Chu YW, Shih T, et al. Drug interaction potential of trastuzumab emtansine (T-DM1) combined with pertuzumab in patients with HER2-positive metastatic breast cancer. *Curr Drug Metabol* 2012; 13:911-22; PMID:22475266; <http://dx.doi.org/10.2174/138920012802138688>
  43. Lu J, Pu J, Lu X, Fu H, Wei M, Yang G. beta-Diketone modified trastuzumab: a next-generation of Herceptin for resistant breast cancer cells? *Med Hypotheses* 2012; 79:602-4; PMID:22922054; <http://dx.doi.org/10.1016/j.mehy.2012.07.030>
  44. Abdiche Y, Malashock D, Pinkerton A, Pons J. Determining kinetics and affinities of protein interactions using a parallel real-time label-free biosensor, the Octet. *Analyt Biochem* 2008; 377:209-17; PMID:18405656; <http://dx.doi.org/10.1016/j.ab.2008.03.035>
  45. Sutherland MS, Sanderson RJ, Gordon KA, Andreyka J, Cervený CG, Yu C, Lewis TS, Meyer DL, Zabinski RF, Doronina SO, et al. Lysosomal trafficking and cysteine protease metabolism confer target-specific cytotoxicity by peptide-linked anti-CD30-auristatin conjugates. *J Biol Chem* 2006; 281:10540-7; PMID:16484228; <http://dx.doi.org/10.1074/jbc.M510026200>